

Stability of Stiffened Cylinders

JOHN M. HEDGEPEETH* AND DAVID B. HALL†
Martin Company, Baltimore, Md.

Design of efficient cylindrical shells for carrying moderate compressive loads leads to the requirement that they be stiffened. The buckling behavior of such stiffened cylinders differs considerably from that of thin monocoque cylinders in several noteworthy respects: 1) Stiffened cylinders are often effectively “thick,” and exhibit large buckle wavelengths. Their strength is consequently influenced little by imperfections and can be predicted accurately by linear buckling analysis. Refined and sophisticated linear analysis thus becomes a powerful design tool. 2) One-sidedness of stringers and rings produces strong interaction between “membrane” and bending forces. Calculations and tests have revealed instances where change of reinforcement from one surface to the other changes buckling strength by a ratio of two or more. 3) Because of the larger, well defined wave form, the strength of stiffened cylinders always depends on the constraint (or lack of it) from adjoining cylinders and domes (or test fixtures), and the resistance to bending moment may appreciably exceed the resistance to uniform load. This paper describes several methods, having varying complexity and versatility, for treating buckling of stiffened cylinders. The determination of the required ring stiffness for preventing general instability is identified as being central to optimum design; commonly used methods of determination are shown to be unreliable. Theoretical and experimental results are compared, and future development is outlined.

Nomenclature

A_{mn}, A_n	= cylinder stiffness matrices
A_r	= area of cross section of a ring
C_r	= ring compliance matrix
E	= modulus of elasticity
F	= matrix defined in Eq. (A4)
G	= shear modulus of elasticity
G_{mn}	= matrix of kinematic relationships, Eq. (10)
H	= constitutive stiffness matrix of cylinder shell, Eq. (2)
H_{ij}	= terms of matrix H
L	= length
M_i	= externally applied moment at i th ring, conjugate to $\partial w / \partial x$
M_x, M_y, M_{xy}	= internal moments, Fig. 1a
N_x, N_y, N_{xy}	= incremental membrane forces, Fig. 1a
\bar{N}_x, \bar{N}_y	= applied membrane forces
$\bar{N}_{x0}, \bar{N}_{x1}$	= components of combined axial and bending loading, Appendix B
R	= cylinder radius, Figs. 1a and 1b
X, Y, Z	= tractions on cylinder or on ring
b	= stringer spacing
m	= number of half-waves in length of cylinder
n	= number of full waves in circumference
t	= thickness of cylinder skin
\bar{t}	= distributed thickness of stringers
t_r	= distributed thickness of rings
u, v, w	= displacements, Fig. 1
x, y, z	= coordinates, Fig. 1
\bar{z}	= radial distance from reference surface to centroid of stringers
z_r	= radial distance from reference surface to centroid of rings
α	= $m\pi/L$ or $(\pi^2/\lambda_x^2)N_{x0}$, Appendix B
β	= m/R or $(\pi^2/2\lambda_r^2)N_{x1}$, Appendix B
γ_{xy}	= incremental shear strain
ϵ_x, ϵ_y	= incremental extensional strains
ν	= Poisson's ratio
θ	= angular coordinate y/R , Fig. 1a
λ_x, λ_y	= distance between buckle node lines
ρ	= radius of gyration (of stringer) about reference surface

ρ_0	= radius of gyration (of stringer or ring) about its own centroid ($\rho^2 = \rho_0^2 + \bar{z}^2$)
$\chi_x, \chi_y, \chi_{xy}$	= incremental curvatures

Introduction

THE use of thin-walled cylinders for carrying compression loads is prevalent in aerospace structures. Because of this, and because of the interesting problems that cylinder stability poses to the analyst, a great deal of research on cylinder buckling has been carried out. Much of this research has been devoted to the problem of large deflections, as a result of the failure of classical deflection theory to predict buckling loads that compare well with experimental results. However, it has been recently realized that most practical efficiently designed cylinders behave in compression in such a way that the small-deflection theory is indeed valid; these cylinders are effectively thick and do not suffer from large knockdowns due to initial imperfections.

Accompanying this realization of the validity of small-deflection theory has been the development of powerful analytical tools for analyzing the linear behavior of complicated structures. Analysts are capable of dealing economically with highly refined models as a result of the high-speed computer replacing the desk calculator. Linear buckling analysis of stiffened cylinders is consequently a fruitful research field.

Recently, a number of interesting phenomena have been treated that are quite important in the design of stiffened cylinders. Among the subjects treated are the effects of one-sidedness of the stiffening elements, the influence of boundary conditions, the effects of combined bending and axial compression, and the proper design of ring stiffeners for preventing general instability. The purpose of this paper is to report on this investigation and to call attention to the important design phenomena.

The emphasis herein is directed toward what is required to achieve good design. The over-all subject is an extremely complex one, and the investigation is, therefore, necessarily incomplete. Paths of future attack are indicated in the Concluding Remarks.

Preliminary Remarks

Stiffened cylinders behave differently from monocoque cylinders in several important respects. These differences

Presented as Preprint 65-79 at the AIAA 2nd Aerospace Sciences Meeting, New York, N. Y., January 25–27, 1965; revision received August 27, 1965.

* Assistant Director of Engineering. Associate Fellow Member AIAA.

† Senior Engineering Specialist. Member AIAA.

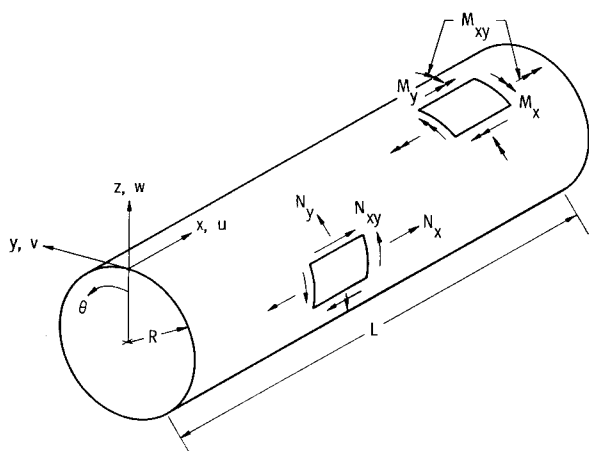


Fig. 1a) Cylinder notation.

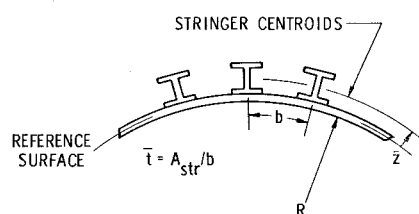


Fig. 1b) Geometry of stringer-stiffened cylinder.

are discussed below as preliminary to the detailed treatment of the buckling of stiffened shells.

Validity of Linear Analysis

Buckling is a particularly serious phenomenon in end-loaded cylinders because postbuckling strength can be small. Small-deflection theory fails for thin monocoque cylinders because its validity is limited to such small buckle amplitude that very slight imperfections may themselves exceed such limits and cause the cylinder, sometimes at a small fraction of buckling load, to go into the postbuckled state and collapse. This sensitivity is associated with the fact that monocoque cylinders have a large variety of buckle-mode patterns, each giving about the same buckling load, and some having very short wavelengths in the circumferential direction. Indeed, calculations show that the circumferential wavelength can be small enough so that the "rise" of the cylinder (as measured from the chord connecting adjacent node lines) is only about 1.5 times the thickness. Initial imperfections in high- R/t cylinders must therefore cause difficulties.

Stiffened cylinders, on the other hand, are effectively low- R/t cylinders if they are designed efficiently. Also, they tend to be much more "selective" in their buckle mode shape and are doubly less susceptible to initial imperfections. Finally, their postbuckling strength tends to drop less drastically than that of thin monocoque cylinders.

These factors all lead to the expectation that linear small-deflection theory is valid for analysis of a large class of stiffened cylinders.

Effects of Length

Thin monocoque cylinders usually buckle in many longitudinal waves. Their strength is therefore virtually independent of length. Longitudinal stiffening lengthens the waves and yields an effectively "shorter" cylinder whose behavior depends strongly on length and the type of boundary conditions. An example is shown in Fig. 2. The curves were calculated by methods discussed later and apply to the extreme cases of fixed ends ($u = v = w = \partial w / \partial x = 0$) and

hinged ends ($v = w = N_x = M_x = 0$). Note that three to four longitudinal half-waves are required before the two curves converge.

Unfortunately the complexity of the boundary conditions for shells prevents the use of "effective length" concepts such as are applied to columns. Careful analysis using actual end conditions is required for reliable results.

Combined bending and axial loading are usually treated by an "effective" end-load concept wherein the maximum compressive stress is assumed to be applied uniformly to the entire perimeter. Thin monocoque cylinders do indeed exhibit this behavior approximately. On the other hand, the comparatively large, and determinate, buckles of stiffened cylinders can lead to an appreciable difference between buckling strength under uniform end load and bending.

Discrete Stiffeners

There are various ways to design stiffened cylinders, but in many cases a "sequential" concept is employed. Since a monocoque cylinder is the most efficient source of membrane stiffness, the purpose of reinforcement is to supply bending stiffness. Bending stiffness per pound increases as the elements get fewer and larger. In typical cylinders, the sequential concept leads to stringers spaced as widely as skin stability will permit and ring frames spaced as widely as stringer stability will permit. The rings are then sized to preclude general instability.

Two important questions immediately arise when this concept is used for designing a cylinder. The first concerns the fact that the procedure assumes implicitly a lack of coupling among the various types of buckling. There is indeed practically no coupling between skin buckling and more general cylinder buckling modes; the concept is therefore valid and the widest possible stringer spacing is best. But, as is discussed below, there is strong coupling between panel buckling (between the rings) and general instability, and the optimum ring spacing may not be the widest possible.

The second question is whether a cylinder thus designed can be analyzed as a continuum (or "orthotropic" shell) or whether a shell plus an actual framework of beams must be treated. As it turns out, stringers are close enough together

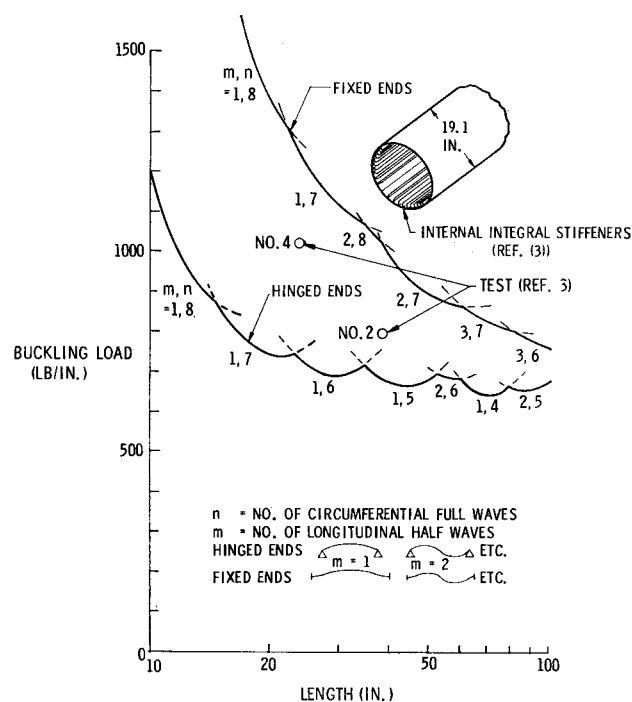


Fig. 2 Effect of length on cylinder buckling.

to be treated as a continuum, whereas rings may or may not be.

Insight into both of these questions is gained by considering the behavior of the greatly simplified problem illustrated in Fig. 3.

An infinitely long column of specified section, supported by beams at undetermined equal intervals, is subjected to a specified end load P . The maximum possible support spacing to preclude buckling between supports is $L_c = \pi(EI/P)^{1/2}$. From Refs. 1 and 2 it is possible to obtain the stiffness K of supports at any lesser spacing L , to prevent general instability. The curve of $k = K/L$ (normalized to k_c at $L = L_c$) is an example. For a considerable part of its length it is practically horizontal, whereas at the right end it rises rapidly.

Now consider the supports as beams, whose moment of inertia is proportional to the square of their area and whose weight W is therefore proportional to $(K)^{1/2}$. The resulting weight $w = W/L$, normalized to w_c at L_c , is shown in Fig. 3. Since the horizontal part of the k curve represents the range in which continuum analysis is valid (the "smeared" stiffness k being constant) and since a constant k implies a decreasing w , it follows immediately that in this case the optimum spacing cannot be within the range of validity of continuum theory. Similarly, the rapid rise at L_c precludes an optimum at that point ("panel-buckling" cutoff).

Each of these conclusions has its obvious extension to cylinders. Care must be taken, however, because of the multiplicity of circumferential buckling modes. The circumferential mode determining the maximum frame spacing (or, for a specified spacing, the minimum shell section) is not necessarily the same as the one for which general instability is critical. Thus the panel-buckling cutoff may sometimes fall to the left of the minimum w (line A-A), or within the range of acceptability of continuum theory (line B-B).

One-Sidedness

Regardless of whether the reinforced cylinder is treated as an orthotropic continuum or as a composite of discrete elements, the treatment is incomplete and incorrect if it fails to include the coupling between bending and extensional forces and deformations resulting from one-sidedness of reinforcement. Calculations, and recent tests made to confirm them,³ have disclosed cases where strength ratios have exceeded 2:1 between otherwise identical cylinders reinforced on opposite sides. The existence of such phenomena has been previously noted,⁴⁻⁶ but their full significance was apparently not appreciated.

General Orthotropic Theory

Because of coupling between membrane and bending properties, and because of the possibility of large circumferential buckle dimensions (including axisymmetric buckles), it is desirable to work from relatively basic relations.

The shell and longitudinal reinforcement, and when permissible the circumferential reinforcement, are treated as an orthotropic continuum. Transverse shear deformations are neglected.

Consecutive Equations

The orthotropic properties of the shells of common types of stiffened cylinders can readily be represented as a 6×6 stiffness matrix:

$$\begin{pmatrix} N_x \\ N_y \\ N_{xy} \\ M_x \\ M_y \\ M_{xy} \end{pmatrix} = H \begin{pmatrix} \epsilon_x \\ \epsilon_y \\ \gamma_{xy} \\ \chi_x \\ \chi_y \\ 2\chi_{xy} \end{pmatrix} \quad (1)$$

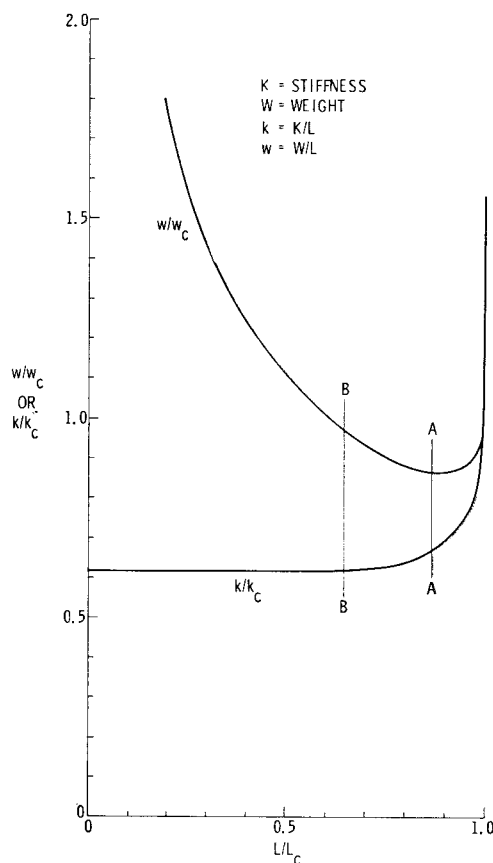


Fig. 3 Characteristics of equally spaced beams supporting a column.

where

$$H = \begin{bmatrix} H_{11} & H_{12} & 0 & H_{14} & H_{15} & 0 \\ & H_{22} & 0 & H_{24} & H_{25} & 0 \\ & & H_{33} & 0 & 0 & H_{36} \\ \text{---} & \text{---} & \text{---} & \text{---} & \text{---} & \text{---} \\ & & & H_{44} & H_{45} & 0 \\ & & & & H_{55} & 0 \\ & & & & & H_{66} \end{bmatrix} \quad (2)$$

The zeros in Eq. (1) follow from the premise that cylinders are orthotropic. In many cases, not all of the remaining terms need be used.

For example, consider a cylinder reinforced by stringers (Fig. 1b). For simplicity, the bending and twisting stiffness of the skin and the twisting stiffness of the stringers have been neglected. Then,

$$\left. \begin{aligned} H_{11} &= Et/(1 - \nu^2)t + E\bar{I} & H_{22} &= Et/(1 - \nu^2)t \\ H_{12} &= \nu Et/(1 - \nu^2)t & H_{33} &= Et/2(1 + \nu)t \\ H_{14} = H_{41} &= -E\bar{I}\bar{z} & H_{44} &= E\bar{I}\rho^2 \end{aligned} \right\} \quad (3)$$

where

$$\bar{I} = A_s/b$$

All other terms are zero. These terms form a 4×4 matrix:

$$H = \frac{Et}{1 - \nu^2} \begin{bmatrix} 1 + \nu & \nu & 0 & -\tau\bar{z} \\ \nu & 1 & 0 & 0 \\ 0 & 0 & (1 - \nu)/2 & 0 \\ -\tau\bar{z} & 0 & 0 & \tau\rho^2 \end{bmatrix} \quad (4)$$

where

$$\tau = (1 - \nu^2)\bar{l}/t$$

The form of Eq. (1) is seen to be ideally suited to a case like this, wherein the stiffnesses of the elements are in parallel and can be assembled directly.

It must be emphasized that Eq. (1) and subsequent development are not universal. For example, the 6×6 stiffness matrix makes no provision for shear deformation in a soft core sandwich, nor, in fact, is a stiffness matrix necessarily the preferred formulation in this case.

Equilibrium and Kinematic Relations

Two adjoint sets of differential equations can be written, one relating external tractions with internal forces, and the other relating internal strains with displacements. In the following forms they will be found to be consistent with the relationships recommended by Sanders⁷:

$$\begin{Bmatrix} X \\ Y \\ Z \end{Bmatrix} = \begin{bmatrix} -(\partial/\partial x) & 0 & -(\partial/\partial y) & 0 \\ 0 & -(\partial/\partial y) & -(\partial/\partial x) & 0 \\ 0 & (1/R) & 0 & (\partial^2/\partial x^2) \end{bmatrix} \begin{Bmatrix} 0 \\ 0 \\ 0 \\ 0 \end{Bmatrix} + \begin{bmatrix} 0 & -(1/2R)(\partial/\partial y) \\ (1/R)(\partial/\partial y) & (3/2R)(\partial/\partial x) \\ (\partial^2/\partial y^2) & (2\partial^2/\partial x \partial y) \end{bmatrix} \begin{Bmatrix} N_x \\ N_y \\ N_{xy} \\ M_x \\ M_y \\ M_{xy} \end{Bmatrix} \quad (5)$$

$$\begin{Bmatrix} \epsilon_x \\ \epsilon_y \\ \gamma_{xy} \\ \chi_x \\ \chi_y \\ \chi_{xy} \end{Bmatrix} = \begin{bmatrix} \frac{\partial}{\partial x} & 0 & 0 \\ 0 & \frac{\partial}{\partial y} & \frac{1}{R} \\ \frac{\partial}{\partial y} & \frac{\partial}{\partial x} & 0 \\ 0 & 0 & \frac{\partial^2}{\partial x^2} \\ 0 & -\frac{1}{R} \frac{\partial}{\partial y} & \frac{\partial^2}{\partial y^2} \\ \frac{1}{2R} \frac{\partial}{\partial y} & -\frac{3}{2R} \frac{\partial}{\partial x} & \frac{2\partial^2}{\partial x \partial y} \end{bmatrix} \begin{Bmatrix} u \\ v \\ w \end{Bmatrix} \quad (6)$$

Note that adjoint matrices are similar to the transposed matrices of matrix algebra except that odd derivatives change sign.

The cylinder, as an elastic structure, resists deformation, and a 3×3 matrix giving the surface forces X, Y, Z required to produce displacements u, v, w is obtained by successively combining Eqs. (5), (1), and (6).

For illustration, consider a specific double sine wave buckle form, which satisfies the foregoing equations, and is valid for calculating the buckling of hinged-end cylinders:

$$\left. \begin{aligned} u &= u^* \cos m\pi x/L \cos ny/R \\ v &= v^* \sin m\pi x/L \sin ny/R \\ w &= w^* \sin m\pi x/L \cos ny/R \\ \phi &= \partial w/\partial x = \phi^* \cos m\pi x/L \cos ny/R \\ \epsilon_x &= \epsilon_x^* \sin m\pi x/L \cos ny/R \\ \epsilon_y &= \epsilon_y^* \sin m\pi x/L \cos ny/R \\ \gamma_{xy} &= \gamma_{xy}^* \cos m\pi x/L \sin ny/R \\ \chi_x &= \chi_x^* \sin m\pi x/L \cos ny/R \end{aligned} \right\} \quad (7)$$

and the eight conjugate force functions. Substitution of Eqs. (7) in Eqs. (5) and (6) transforms them into algebraic equations, and successive matrix multiplication gives

$$\begin{Bmatrix} X^* \\ Y^* \\ Z^* \end{Bmatrix} = Ft/(1 - \nu^2) \begin{bmatrix} \alpha^2(1 + \tau) + \beta^2(1 - \nu)/2 & -\alpha\beta(1 + \nu)/2 & -(\alpha/R)\nu - \alpha^3\tau\bar{z} \\ -\alpha\beta(1 + \nu)/2 & \beta^2 + \alpha^2(1 - \nu)/2 & \beta/R \\ -(\alpha/R)\nu - \alpha^3\tau\bar{z} & \beta/R & 1/R^2 + \alpha^4\tau\rho^2 \end{bmatrix} \begin{Bmatrix} u^* \\ v^* \\ w^* \end{Bmatrix} \quad (8)$$

where

$$\alpha = m\pi/L \quad \beta = n/R$$

In the more general case Eq. (8) becomes

$$\begin{Bmatrix} X^* \\ Y^* \\ Z^* \end{Bmatrix}_{mn} = A_{mn} \begin{Bmatrix} u^* \\ v^* \\ w^* \end{Bmatrix}_{mn} \quad (9)$$

where

$$A_{mn} = G_{mn}^T H G_{mn} \quad (10)$$

G_{mn}^T and G_{mn} are, respectively, the matrices of Eqs. (5) and (6) after the substitution of buckle forms similar to Eqs. (7).

Buckling Forces

Equations such as Eq. (8) give the forces required to deform a cylinder, or, with signs reversed, the resistance of a

cylinder, by virtue of its elastic properties, against deflection. In a loaded cylinder, an additional matrix of force-deflection relations can be found that, in effect, usually add to the effective stiffness of the cylinder when the external loads are tensile and subtracts from it when they are compression or shear. (When, for a particular external load, and for some deflection configuration, the combined stiffness vanishes, that load is a buckling load).

A complete matrix of these buckling forces, beside drawing extensively on large deflection theory, must, in this case, take account of one-sidedness. Most of the terms of such a matrix are small, and the usual practice is to consider only the radial forces associated with change in curvature:

$$Z = \bar{N}_x(\partial^2 w/\partial x^2) + \bar{N}_y[(\partial^2 w/\partial y^2) + (w/R^2)] \quad (11a)$$

One other buckling force is sometimes significant:

$$Y = \bar{N}_x(\partial^2 v/\partial x^2) \quad (11b)$$

Since v^* is usually of the order $(1/n)w^*$ (see Appendix C), the work done by Y is of the order $1/n^2$ compared with that done by Z . Whereas this tangential buckling force is therefore usually secondary, the "column" buckling load of a long slender cylinder (which the methods of this paper are sufficiently fundamental to include) would be found to be exactly twice too high if this force were omitted, since in this mode v^* and w^* are of equal magnitude.

For the example, with $\bar{N}_y = 0$, the following matrix is added to the matrix of Eq. (8):

$$\begin{bmatrix} 0 & 0 & 0 \\ 0 & \alpha^2 N & 0 \\ 0 & 0 & \alpha^2 N \end{bmatrix}$$

where $N = [(1 - \nu^2)\bar{N}_x/Et]$, and the signs have been appropriately adjusted.

Buckling Equations

If the tangential term is neglected to simplify succeeding steps and the eigenvalue problem is solved, the following

buckling formula results:

$$\frac{-\bar{N}_x}{E(t+\bar{t})} = \frac{\bar{t}}{t+\bar{t}} \frac{1}{\gamma^2} \left[\frac{\bar{t}^2}{R^2} - \frac{\bar{t}}{t} \frac{\bar{t}^2}{R^2} (1-\nu^2) \times \right. \\ \left. \frac{1+2n^2 \gamma^2/(1-\nu)}{D} \right] + \frac{2\bar{t}}{t+\bar{t}} \frac{\bar{z}}{R} \frac{-\nu+n^2\gamma^2}{D} + \frac{\gamma^2}{D} \quad (12)$$

[where for \bar{N}_x , tension is positive (hence the minus sign)]

$$\gamma = L/m\pi R$$

[$n\gamma$ is the buckle aspect ratio $\beta/\alpha = \lambda_x/\lambda_y = (L/m)/(\pi R/n)$ and

$$D = 1 + (1-\nu^2)(\bar{t}/t) + 2[1 + (1+\nu)(\bar{t}/t)]n^2\gamma^2 + n^4\gamma^4$$

This equation discloses some interesting facts. The one-sidedness effect is contained in the second term, which shows that internal stringers are most effective when $n = 0$, and external stringers are most effective for multiple waves.

When $n = 0$, the formula (after some manipulation) becomes

$$-N_x = \frac{\pi^2 E}{(L/m)^2} \left(\bar{t}\rho_0^2 + \frac{t'\bar{t}}{t'+\bar{t}} \bar{z}^2 \right) - 2\nu E \frac{\bar{z}}{R} \frac{t'\bar{t}}{t'+\bar{t}} + \\ \frac{(L/m)^2}{\pi^2 R^2} E \left(\frac{t+\bar{t}}{t'+\bar{t}} \right) t$$

where t' is an effective skin thickness $t/(1-\nu^2)$.

The first term is identifiable as the formula for the buckling strength of a wide column. In the last (membrane) term, $E(t+\bar{t})/(t'+\bar{t}) = E'$ can be identified as the orthotropic stiffness $E' = \sigma_y/\epsilon_y$ for the stringer-stiffened sheet making $E' t/R^2$ a readily recognized "foundation modulus."

The middle term is not readily described in familiar terms, but it is interesting to note that for a sufficiently short cylinder it could override the last term and make the cylinder weaker than the corresponding wide column.

Figure 4 shows a plot of buckling load vs the two parameters m and n for a stringer-reinforced cylinder considered in connection with a ring design study described later on. In this plot, m is the abscissa and n provides the family of curves. A cross plot, with only one value of m , is shown in Fig. 5. Here the effect of one-sidedness is graphically apparent. Note the relationship between the cylinder strength and the wide-column strength (the strength of the sheet-stringer combination if it were flat).

The cylinder itself, incidentally, has rather impressive dimensions, being appropriate for use in post-Saturn launch vehicles. The diameter is 866 in. and the length is 361 in. Other dimensions corresponding to the proportions shown in Fig. 6 are as follows. The skin is 0.17 in. thick, and is reinforced by 500 stringers spaced at 5.45 in. Each stringer has an area of 0.865 in.² and a moment of inertia of 1.90 in.⁴ about its own centroid, which is 1.75 in. from the middle surface of the skin. The design load is 12,150 lb/in. and the material is 7075-T6 aluminum alloy.

More General Methods

The simple double-periodic solution of the buckling equations is applicable only to hinged ends and completely uniform cylinders. It is extremely useful in treating panel buckling between rings, but is inadequate for analyzing general instability of nonuniform cylinders with realistic boundary conditions.

There is a class of very practical problems that can be solved by considering more general longitudinal buckle forms while retaining the periodic circumferential pattern. These solutions apply to axially symmetric cylinders, symmetrically loaded, but with the possibility of accounting for end conditions, discrete rings, and any sort of longitudinal variation or discontinuity in the cylinder.

In such a case, the partial differential Eqs. (5, 6, and 11) can be reduced to ordinary differential equations. These ordinary differential equations then can be solved in a variety of ways. Before discussing the various computational procedures, it is desirable to consider the over-all objective.

One more or less standard approach to the solution of buckling problems is exemplified by the analysis of the preceding section in which an unknown buckling load is an "eigenvalue" of the determinant of a matrix generally identifiable as some sort of force-deflection relation. This is in the true spirit of analysis in which the behavior of a given structure is sought.

The designer, on the other hand, is really interested in the question of what structure is needed to carry the design loads. He uses analysis as a tool in determining the load-carrying ability of his trial designs so that he can select the proper one. A more direct approach would be to subject the structure to the design loads and calculate what the properties must be to carry those loads.

In the present case, some of the best methods for treating instability of stiffened cylinder lend themselves to the direct synthesis approach. This is because the most difficult part of the "sequential" concept described in the Preliminary Remarks is the determination of the ring size required to prevent general instability. This ring size can be considered to be the unknown that is sought.

The procedure can be best understood by considering the simpler problem of an axially loaded column with discrete lateral spring supports. The important characteristics of the loaded column itself can be described by an influence coefficient (or compliance) matrix F_{ij} relating the lateral deflections w_i and the lateral spring loads p_j at the support stations. Thus

$$w_i = F_{ij} p_j \quad (13)$$

The springs themselves behave quite simply. If each spring is assumed to have the same stiffness K , then, for the springs

$$w_i = -(1/K)p_i \quad (14)$$

Equating the column deflections with those of the springs yields

$$(1/K)p_i = -F_{ij} p_j \quad (15)$$

Buckling occurs when

$$[F_{ij} + (1/K)\delta_{ij}] = 0 \quad (16)$$

where δ_{ij} is the Kronecker delta (equal to zero for $i \neq j$ and to unity for $i = j$).

Thus, in this simple case, the values of $1/K$ are the (negative) latent roots of the F_{ij} matrix. Note that F_{ij} is dependent on the axial loading, and care must be taken to insure that this load is not so large as to produce buckling between supports.

A similar procedure can be followed (with much more complexity) for the cylinder. Specifically, the problem of determining the required size of ring to reinforce a cylinder becomes one of formulating, say, a compliance matrix relating deflections[‡] to forces for the loaded cylinder at ring stations, and combining it with the corresponding unknown ring compliances to make a vanishing determinant. As in the column case the difficult part is to determine the cylinder compliance.

Trigonometric Series

One comparatively simple procedure for generalizing the longitudinal buckle form is by trigonometric series. Some of the details of the necessary development are assembled in Appendix A. The central feature of this method is that

[‡] Deflections v and w are for beam type rings, plus a rotation for closed rings.

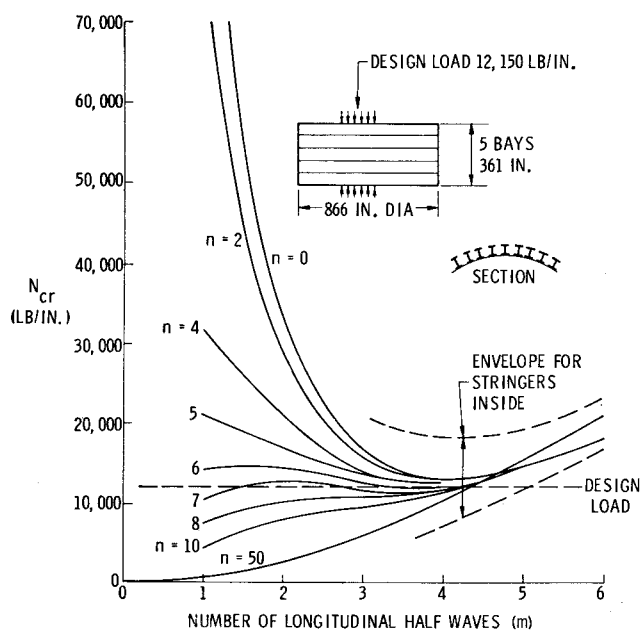


Fig. 4 Cylinder buckling vs mode shape ($b/t=32$), stringers outside.

it allows the rapid calculation of a matrix of compliances at specified locations on a uniform cylinder; these compliances include both elastic properties and "beam column" effects of end load (and internal or external pressure if desired).

This method therefore permits solution of problems in either of the two ways discussed previously: 1) for a specified structure the trigonometric series calculation is repeated using different end loads until one is found for which the actual rings or end constraints make the determinant vanish; 2) for design, the compliance matrix for the cylinder is calculated, using the design load, and rings are then added to make a matrix whose determinant vanishes.

In both cases 1 and 2, the calculation must be repeated for various n 's to find the lowest critical circumferential mode.

The upper curve of Fig. 2, a plot of buckling load vs cylinder length for a cylinder with ends fixed, was obtained by the first procedure. (The lower curve is simply a set of curves for double-periodic buckling.)

Difference Equation Method

Trigonometric series are not profitably adaptable to tapering sections and other irregularities. Hence, for such cases, it appears preferable to concentrate on the development of numerical methods in which the longitudinal section is sampled at discrete points.

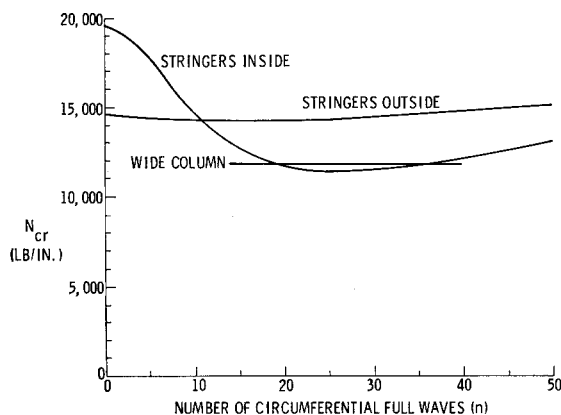


Fig. 5 Panel buckling strength, 5 bays ($b/t=32$, $m=5$).

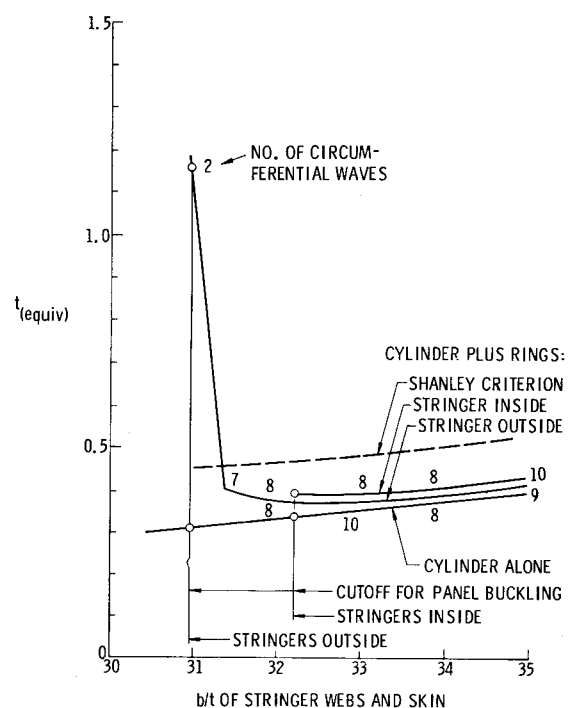


Fig. 6 Cylinder weight vs configuration.

One such procedure, a "difference equation" method, has been developed. The ordinary differential equations (in x) are transformed into difference equations following the general scheme described by Budiansky and Radkowski.⁸ These equations contain the effect of pressure and end load, the end constraints, and the properties of rings.

After these equations are assembled there follow two principal operations which can go in either of two directions:

1) The complete matrix is reduced, by Gaussian elimination, to a smaller matrix of only the equations containing unknowns, which may be a) the end load, if a conventional buckling analysis is sought (and may be limited to only the equations in Z vs w , using the design value of the end load in other equations where its effect is small), or b) the rings, if a design analysis is sought.

2) Values of the unknown to make the determinant of the reduced matrix vanish are found. In case a this may be done by standard "eigenvalue" routines. In case b, where, in general, several properties of a ring (area, moment of inertia, eccentricity) must be related to a single parameter, it must be by trial.

In addition, the buckle shape can (and should) be found as the "eigenvectors" of the matrix.

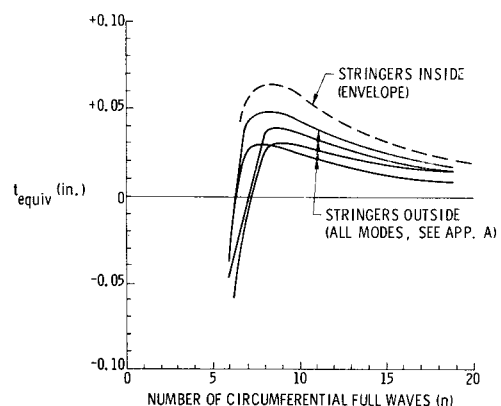


Fig. 7 Ring weight (t_{equiv}) vs n , 5 bays ($b/t=32$).

Table 1 Buckling of cylinders reinforced by longitudinal stringers

Cylinder No. (Ref. (1))		1	2	3	4	5	6
Stiffeners	Type	Integral				Z	
	Location	External	Internal	External	Internal	External	Internal
Length		38 in.		23.75 in.		59 in.	
Radius		9.55 in.				15.8 in.	
Test results	Load No. waves n	1800 lb/in. 6	800 6	2130 7	1030 6	1700 6	1000 6
Calculated (ends fixed)	Load n	2000 7	1010 7	2630 8	1230 7	2200 8	1135 8
Calculated (ends hinged)	Load n	1115 6	689 5	1354 7	725 6	1125 6	735 6

This is a very powerful method and includes auxiliary programs for evaluating the restraints typically provided by domes and adjoining cylinders.

Design Optimization

A simple example of the synthetic design procedure will serve to illustrate the part that it plays in design optimization.

By postulating classical hinged ends ($N_x = M_x = v = w = 0$), and a maximum of four equally spaced rings exerting only radial constraint (so-called "floating" rings), it was feasible to program the trigonometric-series approach on the IBM 1620 computer, and with it to make an optimization study of a typical large launch vehicle intertank section, treated partially in Figs. 4 and 5.

The optimization study compared various ring spacings; typical results are shown in Fig. 6 for a configuration with five 72-in. bays. The abscissa is the b/t ratio of the skin panels and stringer webs and, therefore, determines the stress that the wall can carry without local buckling. For the design load of 12,150 lb/in., the total area in skin and stringers can thus be determined and is indicated by the "weight" thickness of the cylinder alone. The division of this total area between skin and stringers entails a separate optimization, the optimum proportion of area in the skin being somewhat greater for a cylinder than for a wide column. Such optimized proportions were used in constructing Fig. 6.

The range of skin stringer configurations considered in Fig. 6 starts from the lightest cylinder that will not buckle as a panel between rings. The cutoff points are indicated in the figure for both cases of stringers inside and outside.

For each configuration, the ring stiffness required to prevent buckling in all possible modes is then calculated§ (an example is shown in Fig. 7) and, from a family of appropriate ring sections, the corresponding area A_r and equivalent shell thickness $t_r = (m - 1)A_r/L$ of the ring.

In this example certain results may be noted. First, consider the case of external stringers. As was previously pointed out, such cylinders are inherently stronger and, for a given b/t , require less ring reinforcement. The minimum over-all weight is attained at a b/t equal to about 32.5 for which the weight of the cylinder alone is not the lightest and for which the panel buckling strength is somewhat greater than the design load. This behavior is analogous to that previously pointed out for the column with beam supports (Fig. 3).

§ See Eq. (A8) and those following.

A rather spectacular increase in required ring weight is noted as the cutoff for panel buckling is approached. This is probably because the flatness of the panel buckling strength curve for external stringers (Fig. 5) allows the critical general instability mode to occur for $n = 2$; rings are not very effective at such low values of n .

For internal stringers, the situation is somewhat different. The minimum total weight is attained at the panel buckling cutoff. This apparent disagreement with the column results in Fig. 3 arises from the fact that the panel buckling strength for the circumferential wavelength for general instability ($n = 8$) is, as shown in Fig. 5, considerably greater than the panel buckling strength minimized with respect to n . The situation is therefore analogous to the region to the left of line A-A in Fig. 3. Indeed, the panel strength for $n = 8$ is

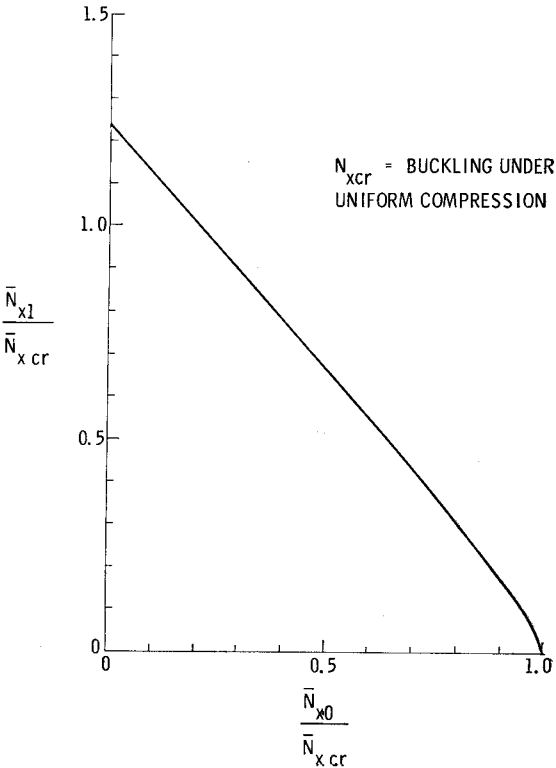


Fig. 8 Typical interaction curve, corrugated cylinder with internal rings.

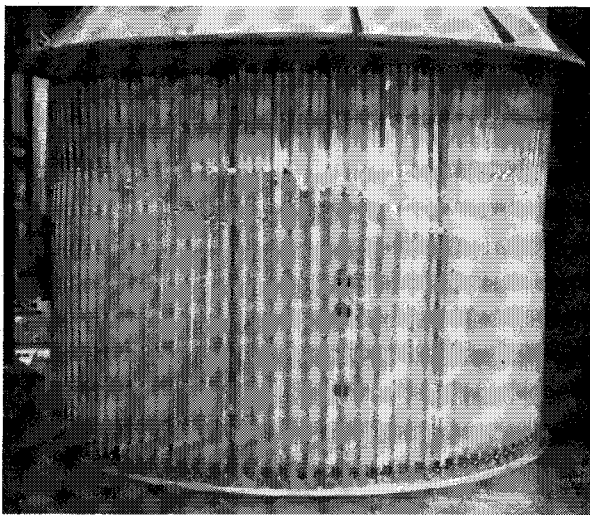


Fig. 9 Buckled $\frac{1}{4}$ -scale test cylinder in test fixture.

probably high enough to be analogous to line B-B and, hence, to allow accurate analysis with orthotropic theory by "smearing" out the rings.

Also shown in Fig. 6 is the weight that would be obtained if the rings were sized by the often used Shanley criterion.⁹ If this criterion were employed, the minimum total weight would be attained at panel-buckling cutoff. For internal stringers, this procedure would yield somewhat conservatively sized rings. For external stringers, however, the rings would be somewhat unconservative. A much more serious deficiency, in an actual practical design, will be cited later.

Combined Bending and Axial Load

By retaining the simple assumptions of a single sine wave with respect to longitudinal buckle shape, but going to trigonometric series in a circumferential direction, it is possible to obtain useful information concerning cylinder buckling under nonuniform end load. Details of the procedure for loadings of the form $\bar{N}_x = \bar{N}_{x0} + \bar{N}_{x1} \cos \theta$ are outlined in Appendix B. Significant results are presented in Fig. 8, which shows an interaction curve between compression and bending. As can be seen, the resistance to bending for the example is about 25% higher than the resistance to compression. This is a considerably higher ratio than obtained for monocoque cylinders.¹⁰ Also, the interaction curve has a vertical tangent at the abscissa; hence, a small amount of bending has little effect on the compression capability.

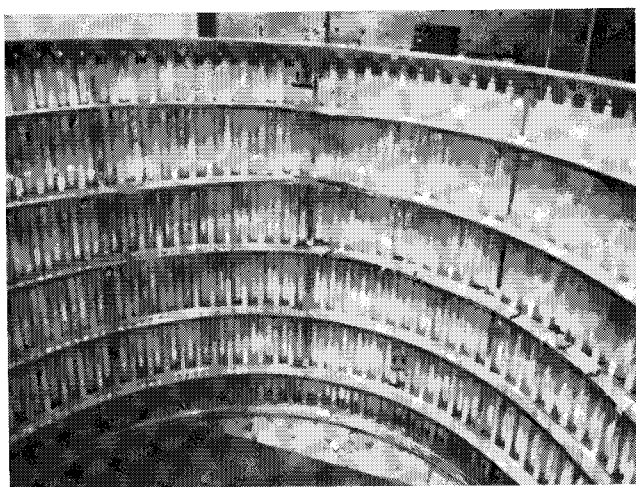


Fig. 10 Internal view of buckled $\frac{1}{4}$ -scale cylinder.

Comparison with Tests

Stringer-Stiffened Cylinders

The first effort to verify the theories under development was by comparing them with the cylinder tests reported by Peterson and Dow.¹¹ These cylinders were internally reinforced by z-stringers and tested flat-ended in compression. Attempts to estimate an effective column length were unsuccessful, but the previously described trigonometric series analysis for representing flat ends gave quite good agreement.

In order to investigate the one-sidedness effect, an investigation was conducted at NASA Langley Research Center (LRC) to repeat and extend these previous tests, this time using duplicate cylinders, half of them with internal stringers and half with external stringers. These tests and their results are reported in Ref. 3 and a summary comparing calculated buckling loads with them is given in Table 1. Two of the cylinder test results are also plotted in Fig. 2.

Although the calculated buckling loads, in general, are several percent higher than the measured ones, the results obviously correlate much better (and more consistently) than they would if the one-sidedness effect were ignored or if an effective-length concept were employed. The agreement is quite good as compared to that obtained in previous studies. The remaining discrepancies might be due to inaccuracies in the boundary conditions. Recent studies (Ref. 13, for instance) have shown that "slippery" ends ($N_{xy} = 0$) cause a marked decrease in the buckling strength.

One interesting result is noted in Table 1: the buckled shape of the failed cylinders was invariably different from the calculated buckling mode (n is smaller). This phenomenon has been observed by Tennyson¹² by means of high speed photoelastic photography.

Ring-Stiffened Corrugated Cylinders

Dealing with cylinders in the manner described in this paper gives considerable insight into their nature and behavior. At a rather early stage it became apparent that corrugated cylinders form a special class of such structures. The circumferential extensional stiffness of corrugations is negligible (typically less than $\frac{1}{1000}$ of longitudinal or shear stiffness), and a corrugated cylinder consequently cannot act as a shell at all until reinforced by rings; the action of the rings is, in turn, rather special.

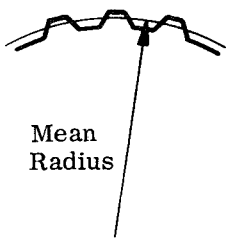
For example, floating rings, such as were considered in the analysis of the large stiffened cylinders discussed previously, would not reinforce a corrugated cylinder at all. Failure would be in the mode $w = w^*(x) \cos \theta$, $u = v = 0$. It is readily ascertainable that in this mode, each corrugation buckles as a column the full length of the cylinder (with appropriate end conditions), whereas every cross section, guided but not otherwise constrained by the floating rings, remains a perfect circle.

Corrugated sheets are otherwise very attractive as cylinder walls since they are one of the most efficient forms of wide column, and they are, in fact, sometimes used for this purpose.

A series of ring-stiffened corrugated cylinders has been built and tested by Boeing as part of the Saturn V development program under the direction of NASA Marshall Space Flight Center (MSFC). As examples, photographs of the exterior and interior of a buckled quarter-scale model of the intertank section of the first stage are shown in Figs. 9 and 10.

The first of the specimens was designed by conventional procedures with the local crippling strength and inter-ring column strength of the corrugations both approximately equal to the design load, and with a ring moment of inertia as given by a usually conservative empirical formula.⁹ This cylinder failed, by general instability, at approximately two thirds of design load. A second cylinder, with rings approximately twice as stiff, failed, also by general instability,

Table 2 Ring stiffened corrugated cylinder, general instability failure

Cylinder Identification		1/8 Scale No. 1	1/8 Scale No. 2	1/8 Scale No. 9	1/4 Scale No. 1
 Mean Radius	Radius (in.)	24.7	24.7	24.7	49.4
	Corrugated depth (in.)	0.44	0.44	0.44	0.87
	Corrugated pitch (in.)	1.43	1.03	1.43	2.85
	Corrugated thickness (in.)	0.020	0.019 to 0.020	0.025	0.041
Cylinder length (in.)		33	33	33	69.6
Ring spacing (in.)		6.38	6.38	6.38	12.37
Ring area (in. ²)		0.040	0.121	0.121	0.180
Ring moment of inertia (in. ⁴)		0.0050	0.0104	0.0104	0.286
Ring eccentricity \bar{Z} (in.)		-0.73	-0.53	-0.53	-1.98
Failing load (lb/in.) test		845	1125	1450	2120
Failing load, calculated, ends simply supported		693	1175	1380	1920
Failing load, calculated, ends fixed		895	1330	1570	2360

at the design load. Additional cylinders, with rings about four times as stiff, failed at about the same load but by local crippling or, with slightly thicker corrugations, by panel instability, i.e., as columns between rings. Two other cylinders failed by general instability, including the quarter-scale model shown in Figs. 9 and 10.

Calculations have been made to compare the predictions of the methods of analysis of this paper with the test results. Since a discrete-ring analysis for corrugated cylinders had not been programed, it was necessary to treat the rings as part of an orthotropic cylinder; this introduced some error in all but the first specimen, for which the buckle length appreciably exceeded the ring spacing.

Cylinder data and results are presented in Table 2 for those cylinders that failed by general instability. (The identification numbers refer to NASA-MSFC designation.) Both fixed-end and hinged-end theoretical results are shown. The ends of the cylinders are actually somewhere between fixed and hinged. Comparison of the experimental and theoretical results lends support to the validity of the theoretical methods.

Bending Tests

The methods developed in this report are not sufficiently general to permit simultaneous consideration of bending moment and end constraint. It appears, however, that buckles produced by bending moment, which are localized on one side of the cylinder, may, as a result, be more localized longitudinally as well.

Buckling stress calculated by the method of Appendix B has been compared directly with measured failing load for three ring-stiffened corrugated cylinders loaded in pure bending. One of these was a duplicate of the 1/8-scale no. 1 cylinder of Table 2; the other two were larger cylinders tested at the NASA-LRC.

In all three cases the measured and calculated results agreed within 5%. Since the ends of the cylinders were restrained in all of the cases, this close agreement actually leaves a question as to whether these results fully validate the method. The answer must await a valid analysis of a fixed-end cylinder in bending.

Concluding Remarks

The main propositions of this paper are 1) that most practical stiffened cylinders will fall within the class of structures for which small deflection theory adequately accounts for buckling, 2) that this fact automatically opens the door to a host of powerful analytical methods for predicting strength, and 3) that the analysis of every cylinder should include recognizing and accounting for all significant aspects of its behavior, and correctly appraising every approximation.

The validity of these propositions has been demonstrated in such ways as the prediction of strengths differing more than 100% in cylinders formerly regarded as identical, and the correct prediction of a strength deficiency of 30% in a corrugated cylinder designed by supposedly conservative criteria. Ultimate implementation of the third proposition extends considerably beyond the topics covered in the paper.

Treatment of external or internal pressure is substantially the same as that of end load. Combination of pressure with plasticity effects raises some important questions. Under a combination of internal pressure and compressive end load, the shell is especially susceptible to plastic straining because of Poisson effects. Indeed, the skin must be made thicker than that required for hoop tension only.

For a low structural index, or for other reasons, a cylinder design may be desired in which skin or "web" elements pre-buckle at less than design loads. Finding the crippling strength of assemblages of such elements is itself an empirical

art. Furthermore, to apply the approaches of this paper, one must determine the effective elastic properties to use in the H matrix [Eq. (4)]. These would characteristically take the form, for example, of extensional stiffness in two directions and shear stiffness of skin buckled between stringers under the action of compressive longitudinal load. Although it is possible to make reasonable or conservative estimates in such circumstances, it is not to be expected that accurate strength predictions can be made for cylinders of this kind without considerable study and gathering of data. The work of Stein¹⁴ on postbuckling behavior of plates furnishes a start in this direction.

Optimization, explained in this paper by a simple example, will more generally involve optimizing for an envelope of design conditions as described, for example, in Ref. 15. Applying these techniques is a desirable direction of progress. In addition, means must be devised for handling more efficient types of structural elements such as closed-section rings.

In a majority of applications, the design loading will involve a combination of bending and end load. The methods developed thus far will not, in general, give results of the desired accuracy, since they cannot simultaneously account for bending and general end conditions. Thus, some sort of two-dimensional analysis will be needed. By analogy with the various one-dimensional analyses heretofore considered, it is expected that a double-trigonometric series approach will be quickest but of limited use, and that the ultimate solution will be by a network analysis.

The latter is quite attractive in principle. For example, bending beyond the proportional limit destroys the axial symmetry of elastic properties. Such a general method could also be applied in other nonuniform cases such as the portion of a cylinder in which engine loads applied through longerons are diffusing into the rest of the cylinder.

$$\begin{pmatrix} X_i \\ Y_i \\ Z_i \\ M_i \end{pmatrix}_n = \begin{bmatrix} \cos ny/R & 0 \\ 0 & \sin ny/R \\ 0 & 0 \\ 0 & 0 \end{bmatrix}$$

From a computation standpoint such a method appears rather formidable. Suppose that symmetry permits con-

$$\begin{pmatrix} X \\ Y \\ Z \end{pmatrix}_n = \sum_{m=0}^{\infty} \begin{bmatrix} \cos m\pi x/L \cos ny/R & 0 \\ 0 & \sin m\pi x/L \sin ny/R \\ 0 & 0 \end{bmatrix} \begin{pmatrix} X^* \\ Y^* \\ Z^* \end{pmatrix}_{mn} \quad (A2)$$

sidering only half the circumference. Then the number of circumferential buckles will be n , and the number of circumferential divisions should be at least three or four times n , typically about 30. For some short cylinders 20 longitudinal divisions might be sufficient, giving a network of a minimum of about 600 points. If a displacement type analysis were used, three displacements and two rotations per point would give a 3000-order matrix, to reduce to a 600-order eigenvalue determinant. Matrices of these sizes and even larger can be handled by present computers but not very economically.

It is the belief of the authors that progress in all these directions should be maintained in order that our understanding and ability to properly analyze keep up with the predictable advances in computer technology.

$$F_m = \begin{bmatrix} \vdots & \cos m\pi x_i/L & 0 \\ \dots & 0 & \sin m\pi x_i/L \\ \vdots & 0 & 0 \end{bmatrix}$$

Appendix A: Buckling Analysis by Trigonometric Series

For cylinders uniform except for a finite number of discrete rings and with end conditions of which at least two at each end can be identically satisfied by all the terms, trigonometric series provide a particularly quick means of calculating cylinder buckling. Trigonometric series can be adapted to cases not meeting all of these restrictions but with diminishing profit.

Two relatively simple applications referred to in the paper are described in this appendix: a simply supported orthotropic cylinder with discrete rings and an orthotropic cylinder with fixed ends.

Simply Supported Cylinder with Discrete Rings

Although basic cylinder properties exemplified by Eq. (9) are in the form of a stiffness matrix, it now becomes necessary to turn to "compliance" or "flexibility" force-deflection relations at ring stations. This is because it is relatively straightforward to resolve a force at a station into trigonometric components and then to calculate the deflections at that and other stations by a summation of the resulting trigonometric components of deflection. Unknown ring compliances can be combined with this to give a matrix whose vanishing determinant determines the critical ring compliance for buckling.

Amplitudes of all singly periodic variables (in n), as well as doubly periodic variables as in Eq. (7), will be identified by an asterisk (*). The variables associated with a ring at $x = x_i$ will be identified by subscripts i and doubly periodic variables by the subscripts mn . We consider the n th circumferential buckling mode.

The forces to be applied at the i th ring station may be, in the most general case,

$$\begin{pmatrix} 0 & 0 \\ 0 & 0 \\ \cos ny/R & 0 \\ 0 & \cos ny/R \end{pmatrix} \begin{pmatrix} X_i^* \\ Y_i^* \\ Z_i^* \\ M_i^* \end{pmatrix}_n \quad (A1)$$

In general, the surface loading on a cylinder can be given by the following Fourier series:

$$\begin{pmatrix} X \\ Y \\ Z \end{pmatrix}_n = \sum_{m=0}^{\infty} \begin{bmatrix} \cos m\pi x/L \cos ny/R & 0 \\ 0 & \sin m\pi x/L \sin ny/R \\ 0 & 0 \end{bmatrix} \begin{pmatrix} X^* \\ Y^* \\ Z^* \end{pmatrix}_{mn} \quad (A2)$$

The concentrated forces defined in Eq. (A1) may be resolved into trigonometric components [Eq. (A2)] by the regular rules for forming trigonometric series, admissible for further operating even though the series for the loading itself is divergent. These components are

$$\begin{pmatrix} X^* \\ Y^* \\ Z^* \end{pmatrix}_{mn} = \frac{2}{L} \frac{F_m}{1 + \delta_{0m}} \begin{pmatrix} \vdots \\ X_i^* \\ Y_i^* \\ Z_i^* \\ M_i^* \\ \vdots \end{pmatrix} \quad (A3)$$

where δ_{0m} is the Kronecker delta, unity for $m = 0$ and zero for all other values of m , and the partitioned form of the right-hand column matrix signifies that the complete matrix includes all ring stations; and where

$$\begin{pmatrix} 0 & 0 \\ 0 & 0 \\ \sin m\pi x_i/L & m\pi/L \sin m\pi x_i/L \end{pmatrix} \vdots \quad (A4)$$

Now, the deflections at station x_i are expressed by substituting x_i in appropriate Fourier series made up of terms like those in Eq. (7). For generality, a fourth set of equations for the slope $\phi = \partial w / \partial x$ is added.

$$\begin{pmatrix} \dots \\ u_i^* \\ v_i^* \\ w_i^* \\ \phi_i^* \\ \dots \end{pmatrix} = \sum_{m=0}^{\infty} F_m^T \begin{pmatrix} u^* \\ v^* \\ w^* \end{pmatrix}_{mn} \quad (\text{A5})$$

Note that the operator in (A5) is found to be transpose of (A4). The Fourier components for the deflection on the right of Eq. (A5) can be found in terms of the Fourier components of the loading by means of the analysis derived in the section entitled General Orthotropic Theory. Let \bar{A}_{mn} denote the matrix obtained when the matrix A_{mn} defined in Eq. (10) is properly augmented by the buckling forces of Eq. (11). Then,

$$\begin{pmatrix} u^* \\ v^* \\ w^* \end{pmatrix}_{mn} = \bar{A}_{mn}^{-1} \begin{pmatrix} X^* \\ Y^* \\ Z^* \end{pmatrix}_{mn} \quad (\text{A6})$$

The required deflection influence matrix can now be assembled by multiplying together (A5, A6, and A3):

$$\begin{pmatrix} \dots \\ u_i^* \\ v_i^* \\ w_i^* \\ \phi_i^* \\ \dots \end{pmatrix}_n = B_n \begin{pmatrix} \dots \\ X_i^* \\ Y_i^* \\ Z_i^* \\ M_i^* \\ \dots \end{pmatrix}_n \quad (\text{A7})$$

where

$$B_n = \frac{2}{L} \sum_{m=0}^{\infty} F_m^T \bar{A}_{mn}^{-1} \frac{F_m}{1 + \delta_{0m}}$$

For rings that act only in their plane, the matrix A_{mn}^{-1} can be condensed to 2×2 by setting $X = 0$ in Eq. (A6), and columns relating to X and M can be deleted from F_m . For the floating rings, A_{mn}^{-1} condenses to a single term and Eq. (A7) reduces to an equation between w 's and Z 's.

For rings acting only in their plane, Eqs. (A7) and (C1) can be combined by requiring that the cylinder and the rings have consistent deflections. Equating the two deflection matrices gives (note the sign change made in order that action and reaction oppose each other)

$$\left(B_n + \begin{bmatrix} \dots & \dots & \dots & \dots \\ \dots & C_r & 0 & \dots \\ \dots & 0 & C_r & \dots \\ \dots & \dots & \dots & \dots \end{bmatrix}_n \right) \begin{pmatrix} \dots \\ Y_i^* \\ Z_i^* \\ Y_{i+1}^* \\ Z_{i+1}^* \\ \dots \end{pmatrix} = 0 \quad (\text{A8})$$

To make the determinant of the matrix of Eq. (A8) vanish, it is necessary to calculate the matrices C_r for a succession of ring sizes until the correct size is found by trial.

For floating rings the problem is much simpler. If only bending is considered, Eq. (C1) reduces to

$$w_n^* = [R^4/EI_r(n^2 - 1)^2]Z_n^* \quad (\text{A9})$$

and the expression $[R^4/EI_r(n^2 - 1)^2]$ becomes the undetermined eigenvalue of the equation corresponding to (A8).

For a given family of rings this can be transformed into an equivalent "weight thickness" t_r . For each value of n there will be as many eigenvalues as there are rings. The four curves of Fig. 7 show the results of a typical calculation for a cylinder with four rings. Negative values ($n \leq 6$) indicate that in these modes the cylinder would be stable without rings, and negative ring compliance would be re-

quired to make the cylinder buckle. Examination of Fig. 4 confirms that the cylinder is in fact stable under the design load for all buckle lengths (L/m) when $n \leq 6$.

Cylinder with Fixed Ends

Trigonometric series with terms in the form of Eq. (7) identically satisfy two of the conditions of end fixity $v \equiv w \equiv 0$, but do not satisfy the conditions $u = \partial w / \partial x = 0$. It can be shown that the buckling load for a cylinder with fixed ends can be defined as the load under which circumferentially periodic end forces N_x and M_x produce no deflection u or $\partial w / \partial x$.

Although the internal forces N_x and M_x vanish, the same result is achieved by applying external forces X and M indefinitely close to the end; Eq. (A3) applies equally well to this case. In fact, all equations (A1-A8) are applicable. An effective ring station is assumed at each end. These rings are assumed to be infinitely stiff and therefore to have zero compliance. The only essential departure from the preceding problem is that, since this is an analytical instead of a design problem, the end load \bar{N}_x is the unknown, and the determinant B_n is made to vanish by trying successive values of \bar{N}_x in Eq. (A6).

Appendix B: Buckling of Cylinders in Bending

Let the end load be

$$\bar{N}_x = \bar{N}_{x0} + \bar{N}_{x1} \cos \theta \quad (\text{B1})$$

Let the buckled shape be

$$\begin{cases} u = \cos \pi x / \lambda_x (u_0 + u_1 \cos \theta \dots + u_n \cos n \theta \dots) \\ v = \sin \pi x / \lambda_x (v_1 \sin \theta \dots + v_n \sin n \theta \dots) \\ w = \sin \pi x / \lambda_x (w_0 + w_1 \cos \theta \dots + w_n \cos n \theta \dots) \end{cases} \quad (\text{B2})$$

Tractions associated with the buckled shape will be

$$\begin{cases} X = \cos \pi x / \lambda_x (X_0 + X_1 \cos \theta \dots + X_n \cos n \theta \dots) \\ Y = \sin \pi x / \lambda_x (Y_1 \sin \theta \dots + Y_n \sin n \theta \dots) \\ Z = \sin \pi x / \lambda_x (Z_0 + Z_1 \cos \theta \dots + Z_n \cos n \theta \dots) \end{cases} \quad (\text{B3})$$

The buckling forces will be radial and tangential. The radial buckling force is

$$\begin{aligned} Z = \bar{N}_x (\partial^2 w / \partial x^2) = -(\pi^2 / \lambda_x^2) \sin \pi x / \lambda_x \times \\ [\bar{N}_{x0}(w_0 + w_1 \cos \theta \dots + w_n \cos n \theta \dots) + \\ \bar{N}_{x1}(w_0 \cos \theta + w_1 \cos^2 \theta \dots + w_n \cos \theta \cos n \theta \dots)] \end{aligned} \quad (\text{B4})$$

The tangential buckling forces are assumed to be negligible.

The coefficients of \bar{N}_{x1} in Eq. (B4) can be manipulated to eliminate products of cosines and transform Eq. (B4) into an ordinary series. These transformations are

$$\begin{aligned} w_0 \cos \theta &\equiv w_0 \cos \theta \\ w_1 \cos^2 \theta &= \frac{1}{2} w_1 (1 + \cos 2\theta) \\ w_n \cos \theta \cos n \theta &= \frac{1}{2} w_n [\cos(n-1)\theta + \cos(n+1)\theta] \end{aligned} \quad (\text{B5})$$

For any mode (buckle length λ_x , buckle width $\pi R/n$), there is an elastic stiffness matrix the same, except for some changes in notation, as Eq. (9):

$$\begin{pmatrix} X_n \\ Y_n \\ Z_n \end{pmatrix} = A_n \begin{pmatrix} u_n \\ v_n \\ w_n \end{pmatrix} \quad (\text{B6})$$

Since only buckling forces Z_n are considered, one can set $X_n = Y_n = 0$ and condense Eq. (B6) to a single equation:

$$Z_n = B_n w_n \quad (\text{B7})$$

Equations (B4) and (B7) can be combined to give total load vs deflection. Let

$$(\pi^2 / \lambda_x^2) \bar{N}_{x0} = \alpha \quad (\pi^2 / 2 \lambda_x^2) \bar{N}_{x1} = \beta$$

$$\{0\} = \begin{Bmatrix} Z_0 \\ Z_1 \\ Z_2 \\ Z_3 \\ \dots \end{Bmatrix} = \begin{bmatrix} \frac{1}{2}(B_0 + \alpha) & \beta & & & \\ \beta & B_1 + \alpha & & & \\ 0 & \beta & & & \\ 0 & 0 & & & \\ \dots & \dots & \dots & \dots & \dots \end{bmatrix} \begin{Bmatrix} 0 \\ 0 \\ \beta \\ B_2 + \alpha \\ \beta \\ \dots \end{Bmatrix} + \begin{bmatrix} 0 & 0 & \dots \\ 0 & 0 & \dots \\ \beta & \beta & \dots \\ B_3 + \alpha & \beta & \dots \\ \dots & \dots & \dots \end{bmatrix} \begin{Bmatrix} 2w_0 \\ w_1 \\ w_2 \\ w_3 \\ \dots \end{Bmatrix} \quad (B8)$$

Buckling loads are found from combinations of α and β which make the infinite determinant of Eq. (B8) vanish. For end load alone, $\beta = 0$, and the various buckling modes are given by $\alpha = B_n$.

In solving for β , Eq. (B8) can be made a little more compact by letting $B_n + \alpha = B_n'$. (B_n' can in fact include internal or external pressure if desired.)

Although Eq. (B8) involves an infinite matrix, it turns out that β can be calculated accurately using a finite number of terms, since partial determinants containing large numbers of terms tend to become all positive or all negative for slight changes in the value of β .

The calculation of the determinant of Eq. (B8) is facilitated by using the recursion formula

$$D_{n+1} = B_{n+1}'D_n - \beta^2 D_{n-1} \quad (B9)$$

where D_n is the $(n+1) \times (n+1)$ determinant containing B_n' in the lower right-hand corner. This formula is applied after the first two determinants are calculated:

$$D_0 = \frac{1}{2}B_0' \quad D_1 = \frac{1}{2}B_0'B_1' - \beta^2 \quad (B9a)$$

Appendix C: Ring Stiffeners

Beam-Type Rings

Since beam-type rings for large launch vehicles may be complete built-up beams with flanges, webs, and stiffeners, it may at times be desirable to include shear deformation as well as bending and extensional deformation.

The following formula accounts for these plus attachment compliances. Its compliance matrix may be used as it is [see for example Appendix A, Eq. (A8)] or inverted, depending on the form of cylinder analysis with which it is to be used. Constitutive compliances are $1/EA_r$ for extension, $1/EA_r\rho_0^2$ for bending, and $1/KA_rG$ for shear. Letting $\kappa = E/KG$, the shear compliance becomes κ/EA_r . Tangential and radial attachment compliances are C_y and C_z , and $C_y' = C_y[EA_r(n^2 - 1)^2/R(R + z_r)]$, etc.

Let

$$\begin{Bmatrix} v^* \\ w^* \end{Bmatrix} = C_r \begin{Bmatrix} Y^* \\ Z^* \end{Bmatrix} \quad (C1)$$

where

$$C_r = \frac{R(R + z_r)}{EA_r(n^2 - 1)^2} \begin{bmatrix} C_{22} & C_{23} \\ C_{23} & C_{33} \end{bmatrix}$$

$$\begin{cases} C_{22} = n^2 + (1/\rho_0^2)(R/n + nz_r)^2 + \kappa + C_y' \\ C_{23} = -(n + (1/\rho_0^2)(R + z_r)(R/n + nz_r) + n\kappa) \\ C_{33} = 1 + (1/\rho_0^2)(R + z_r)^2 + n^2\kappa + C_z' \end{cases}$$

Besides the obvious primary extension and bending terms there is one very important coupling term, the off-diagonal term $(1/\rho_0^2)(R + z_r)(R/n + nz_r)$. Every elastic ring under periodic in-plane loading has a neutral axis, usually near the centroid, along which ϵ_y is zero. At this radius $v^* = -w^*/n$ [observed by setting the second of Eq. (6) equal to zero]. It is readily demonstrated that there is another circle along which displacements v vanish, and the radial distance z_0 from the axis of no displacement to the axis of no strain is found to be $z_0 = -R/n^2$. Thus, when the distance z_r from shell centroid to ring centroid is equal to z_0 , the coupling term vanishes, and the ring becomes completely ineffective as membrane reinforcement. In the case of corrugated cylinders with internal rings this leads to buckling in relatively few

waves and greatly increases the required ring moment of inertia.

For buckling modes $n = 0$ and $n = 1$, which will sometimes be encountered, there are equilibrium restrictions that require modification of Eq. (C1). (For $n > 1$, Y and Z are independently self equilibrating.) The conditions are

$$n = 0 \quad \begin{cases} Y = 0 \\ Z = \text{const} \end{cases} \quad n = 1 \quad \begin{cases} Y = Y^* \sin y/R \\ Z = Z^* \cos y/R \\ Y^* = Z^* \end{cases}$$

For $n = 0$, Eq. (C1) reduces to

$$w = [R(R + z_r)/EA_r + C_z]Z \quad (C2)$$

and the inverse is simply the reciprocal. For $n = 1$, there is a single loading $Y^* = Z^*$, and a deflection relative to the cylinder $v^* + w^*$:

$$v^* + w^* = [R(R + z_r)/EA_r + C_y + C_z]Z^* \quad (C3)$$

$$\begin{Bmatrix} Y^* \\ Z^* \end{Bmatrix} = \{1/[R(R + z_r)/EA_r + C_y + C_z]\} \begin{bmatrix} 1 & 1 \\ 1 & 1 \end{bmatrix} \begin{Bmatrix} v^* \\ w^* \end{Bmatrix} \quad (C4)$$

References

- ¹ Budiansky, B., Seide, P., and Weinberger, R. A., "The buckling of a column on equally spaced deflectional and rotational springs," NACA TN 1519 (1948).
- ² Budiansky, B. and Seide, P., "Compressive buckling of simply supported plates with transverse stiffeners," NACA TN 1557 (1948).
- ³ Card, M. F., "Preliminary results of compression tests on cylinders with eccentric longitudinal stiffeners," NASA TM X-1004 (1964).
- ⁴ Hedgepeth, J. M., "Design of stiffened shells in axial compression, collected papers on instability of shell structures—1962," NASA TN D-1510, pp. 77–83 (1962).
- ⁵ Van der Neut, A., "General instability of orthogonally stiffened cylindrical shells, collected papers on instability of shell structures—1962," NASA TN D-1510, pp. 309–321 (1962).
- ⁶ Baruch, M. and Singer, J., "Effect of eccentricity of stiffeners on the general instability of stiffened cylindrical shells under hydrostatic pressure," J. Mech. Eng. Sci. 5, 23–27 (March 1963).
- ⁷ Sanders, J. L., Jr., "An improved first-approximation theory for thin shells," NASA TR R-24 (1959).
- ⁸ Budiansky, B. and Radkowski, P. P., "Numerical analysis of unsymmetrical bending of shells of revolution," AIAA J. 1, 1833–1842 (1963).
- ⁹ Shanley, F. R., "Simplified analysis of general instability of stiffened shells in pure bending," J. Aeronaut. Sci. 16, 590–592 (1949).
- ¹⁰ Seide, P. and Weingarten, V. I., "On the buckling of circular cylindrical shells under pure bending," Trans. Am. Soc. Mech. Engrs. 28, 112–116 (1961).
- ¹¹ Peterson, J. P. and Dow, M. B., "Compression tests on circular cylinders stiffened longitudinally by closely spaced z-section stringers," NASA Memo 2-12-59L (March 1959).
- ¹² Tennyson, R. C., "Buckling of circular cylindrical shells in axial compression," AIAA J. 2, 1351–1353 (1964).
- ¹³ Hoff, N. J., "The effect of the edge conditions on the buckling of thin-walled circular cylindrical shells in axial compression," Stanford Univ. Dept. of Aerospace Engineering Research SUDAR 205, U.S. Air Force Office of Scientific Research, AF OSR 64-1724 (August 1964).
- ¹⁴ Stein, M., "Behavior of buckled rectangular plates," J. Eng. Mech. Div., 86, EM2, 59–76 (1960).
- ¹⁵ Schmit, L. A., Jr. and Fox, R. L., "An integrated approach to structural synthesis and analysis," AIAA 5th Structures and Materials Conference (American Institute of Aeronautics and Astronautics, New York, 1964), pp. 294–315.